

Distributed Multi-Agent Deep Reinforcement Learning Framework for Whole-building HVAC Control

Vinay Hanumaiah
vinayha@amazon.com
Amazon Web Services
Santa Clara, CA, USA

Sahika Genc
sahika@amazon.com
Amazon Web Services
Seattle, WA, USA

ABSTRACT

It is estimated that about 40%-50% of total electricity consumption in commercial buildings can be attributed to Heating, Ventilation, and Air Conditioning (HVAC) systems. Minimizing the energy cost while considering the thermal comfort of the occupants is very challenging due to unknown and complex relationships between various HVAC controls and thermal dynamics inside a building. To this end, we present a multi-agent, distributed deep reinforcement learning (DRL) framework based on Energy Plus simulation environment for optimizing HVAC in commercial buildings. This framework learns the complex thermal dynamics in the building and takes advantage of the differential effect of cooling and heating systems in the building to reduce energy costs, while maintaining the thermal comfort of the occupants. With adaptive penalty, the RL algorithm can be prioritized for energy savings or maintaining thermal comfort. Using DRL, we achieve more than 75% savings in energy consumption. The distributed DRL framework can be scaled to multiple GPUs and CPUs of heterogeneous types.

KEYWORDS

Reinforcement learning, deep learning, HVAC optimization, machine learning

1 INTRODUCTION

Buildings account for 40% of total energy consumption, 70% of total electricity, and 30% of carbon emissions in the United States [18, 22]. HVAC systems account for 50% of the total energy consumption in buildings. The aim of HVAC systems in residential and commercial buildings is to maintain indoor air temperature and air quality. The conventional building HVAC control is rule-based feedback. In this setup, temperature setpoints are set based on certain pre-determined schedules (e.g. day and night time schedules). A simple controller like Proportional-Integral-Derivative (PID) [6] is used for tracking the setpoints. This simple reactive strategy works well to maintain indoor air temperature on a per-zone basis, but would not be optimal for a large building with many thermal zones. The strategy also ignores the effects of external elements like weather. Additional savings in energy can be achieved by intelligently controlling HVAC systems.

Optimal control strategies, such as MPC (Model Predictive Controller) address above limitations by iteratively optimizing an objective function over a finite time horizon. One of the limitations of MPC is the need for accurate models of the environment. The thermal dynamics in a large building is very complex with zones at the periphery having different thermal properties than one in the middle, and similar behavior can be seen with multiple floors in the

building. Moreover, the dynamics of two buildings can be very different depending on the layout, HVAC configurations, and occupancy rates. Modeling these different thermal properties of buildings is difficult and needs to be repeated for a new building. Model-free optimization is preferred in such scenarios and Reinforcement learning (RL) [24] is well suited for model-free optimization. RL directly interacts with an environment, and learns the model through set of actions and corresponding feedback in the form of state changes. DRL incorporates deep learning with RL, allowing agents to make decisions from unstructured input data without manual engineering of the state space. DRL has achieved remarkable success in playing Atari and Go [15]. DRL is especially well suited for model-free RL, where the agent can learn to model the environment by exploring extensively. Ray Rllib [10] is a popular DRL framework, which supports commonly used DRL algorithms.

Since RL algorithms require extensive action-state pairs from an environment to optimize, RL algorithms are usually trained on simulators, as (i) trying those actions in real world could be dangerous, e.g. setting temperature too high or cold in a building, and (ii) collecting the extensive data would take a long time in real world. EnergyPlus [4] is a whole building energy simulation program that models heating, cooling, ventilation, lighting, and water use in buildings. EnergyPlus is commonly used by design engineers and architects, who would like to design for HVAC equipment, or analyzing life cycle cost, or optimize energy performance, etc.

In this paper, we present a co-simulation framework, where DRL algorithms from Ray Rllib will interact with EnergyPlus simulator to arrive at optimal HVAC policy. The co-simulation framework will provide seamless and scalable interface, where observations from EnergyPlus are provided to OpenAI gym environment, which in turn will compute reward. The rewards are collected by Rllib and compute the optimal actions for next time step. These actions are conveyed back to OpenAI gym and is supplied to EnergyPlus. Though this co-simulation framework, EnergyPlus, which is designed to run as single process, is extended Rllib's distributed model to scale for multiple CPUs and GPUs across clusters. This is made possible by using callbacks from EnergyPlus and utilizing queues to synchronize the two softwares. Additionally, we demonstrate setting up multi-zone and multi-agent environments with this framework.

The main contributions of this work are summarized below:

- (1) This paper provides an optimization framework by orchestrating a co-simulation environment between Ray Rllib and EnergyPlus. The framework is highly scalable to using multiple compute instances including CPUs and GPUs.
- (2) The above framework uses standard OpenAI gym, which is customizable, and supports multiple DRL algorithms (all

that is supported by RLlib). We demonstrate setting up multi-zone control and multi-agents to control building at different times of the year.

- (3) We conduct experiments for different weather conditions and simulator configurations. We demonstrate the trade-off in training times and rewards w.r.t. energy-temperature penalty coefficient.

1.1 Related Work

The recent literature in HVAC optimization for buildings generally falls in two categories. One that uses MPC, the other uses RL. One of the roadblocks in widespread adoption of MPC is the need for a model [9, 19]. Due to heterogeneity of the buildings, we may need to develop model for each thermal zone [12]. The models could be built based on physics, e.g. EnergyPlus, or based on material characteristics, e.g. computation fluid dynamics models. These models are not control-oriented [1], and although not impossible, it requires considerable work to control these models.

Many DRL based HVAC control methods have been proposed. Wei et al. [25] DRL method based on Deep Q-Network (DQN) [14] was one of the first DRL based control methods to minimize energy consumption, while maintaining temperature in a desired range. Gao et al. [5] proposed a Deep Deterministic Policy Gradients (DDPG) [11] based DRL method to minimize energy consumption and thermal discomfort in a laboratory setting. Similarly, Zhang et al. [26] proposed Asynchronous Advantage Actor Critic (A3C) [13] based control to jointly optimizes energy demand and thermal comfort in an office building.

Some of the works have utilized EnergyPlus to model the building and use it as a simulator to verify the HVAC control methods. Chen et al. [3] validated their work on a large office (16 thermal zones) within EnergyPlus by controlling the temperature setpoints. Moriyama et al. [17] presented a test bed that integrates DRL with EnergyPlus for data center HVAC control. Our work is most similar to this work. One of the limitation of [17] was the co-simulation is not scalable to beyond one core. In this paper, we provide the framework that is highly scalable to multiple cores and multiple nodes.

The rest of the paper is structured as follows: Section 2 covers problem formulation and introduction to EnergyPlus simulator. Section 3 introduces the reader to deep reinforcement learning algorithms for HVAC control. Section 4 presents the results of exploring DRL algorithms with EnergyPlus, and finally we conclude the paper in Section 5.

2 HVAC SYSTEM MODELING OF BUILDINGS

In this section, we will cover the problem formulation, discuss EnergyPlus and reinforcement learning frameworks, and strategies to distribute workloads to speed up computation.

2.1 Problem Formulation

Table 1 lists the nomenclature used in this paper:

The goal of our work is to minimize energy consumption in a building subject to maintaining zone temperatures within the range

Table 1: Nomenclature used in the paper.

Symbol	Description
N_z	Number of thermal zones.
N_d	Number of simulation days.
t_s	Timestep (s)
T_{min}, T_{max}	Minimum and maximum acceptable zone temperature ($^{\circ}$ C), respectively
T_z	Zone z temperature ($^{\circ}$ C), T represents the vector of all zone temperatures.
P_z^h	Heat added to zone z per unit timestep
P_z^c	Heat removed from zone z per unit timestep
P_b	Base energy expenditure (unrelated to zone) per unit timestep, e.g. energy used for lighting, etc.
α	Energy-temperature penalty ratio
T_z^h	Heating setpoint temperature for zone z ($^{\circ}$ C)
T_z^c	Cooling setpoint temperature for zone z ($^{\circ}$ C)
T_e	Outdoor temperature ($^{\circ}$ C)
R_h	Relative humidity (%)
T_{min}^h, T_{max}^h	Minimum and maximum heating setpoint ($^{\circ}$ C), respectively
T_{min}^c, T_{max}^c	Minimum and maximum cooling setpoint ($^{\circ}$ C), respectively

of comfort. The problem can be mathematically stated as follows:

$$\min_{T_z^h(t_s), T_z^c(t_s)} \sum_{t_s=0}^{t_s=N_d} \left[P_b(t_s) + \sum_{z=0}^{z=N_z} P_z^h(T_z^h, t_s) + P_z^c(T_z^c, t_s) \right] \quad (1)$$

$$s.t. \quad T_{min}^h \leq T_z^h(t_s) \leq T_{max}^h \quad \forall z, t_s \quad (2)$$

$$T_{min}^c \leq T_z^c(t_s) \leq T_{max}^c \quad \forall z, t_s \quad (3)$$

$$T_z(t_s) = f_T(\mathbf{T}, T_e, R_h, \mathbf{P}^h, \mathbf{P}^c, t_s) \quad \forall z, t_s \quad (4)$$

$$P_z^h(t_s) = f_{P_h}(\mathbf{T}, T_z^h, t_s), \quad \forall z, t_s \quad (5)$$

$$P_z^c(t_s) = f_{P_c}(\mathbf{T}, T_z^c, t_s), \quad \forall z, t_s \quad (6)$$

$$T_{min} \leq T_z(t_s) \leq T_{max} \quad \forall z, t_s \quad (7)$$

Equation 1 is the objective function, where we minimize the overall energy consumption for all simulation steps and all zones. Power consumed for heating and cooling are described in Equations 5 and 6, respectively. The power consumed is a function of the setpoint, the temperature of all zones. Since temperature of a zone is influenced by other nearby zones, we need temperature of all zones to compute the effective power to bring the temperature of a zone to it's desired range. Similarly, function for computing zone temperatures is dependent on both heating and cooling setpoints, and the temperature of all zones, as described in Equation 4. Note that f_{P_h} , f_{P_c} , and f_T are black-box functions, which are learned by Model-free RL algorithms described in Section 3 as they optimize for reward.

Of the constraints mentioned in Equations 2, 3, and 7, Equation 7 is the constraint on the observed temperatures, while the rest are the constraints on the input variables. Equation 7 presents a challenge in optimizing for algorithms, as solving for hard constraint increases the complexity of the algorithms. Equations 2 and 3 are constraints

on control variables, which are easily handled by limiting the range of input variables. One common way of addressing this issue is by modifying the hard constraint as a soft constraint in the objective with an added penalty coefficient as shown in Equation 8.

$$\min_{T_z^h(t_s), T_z^c(t_s)} \sum_{t_s=0}^{t_s=N_d} \left[P_b(t_s) + \sum_{z=0}^{z=N_z} \left(P_z^h(T_z^h, t_s) + P_z^c(T_z^c, t_s) + \alpha (\max(T_{min} - T_z(t_s), T_z(t_s) - T_{max}, 0))^\lambda \right) \right] \quad (8)$$

$$s.t. \quad T_{min}^h \leq T_z^h(t_s) \leq T_{max}^h, \quad \forall z, t_s \quad (9)$$

$$T_{min}^c \leq T_z^c(t_s) \leq T_{max}^c, \quad \forall z, t_s \quad (10)$$

$$T_z(t_s) = f_T(\mathbf{T}, T_e, R_h, \mathbf{P}^h, \mathbf{P}^c, t_s) \quad \forall z, t_s \quad (11)$$

$$P_z^h(t_s) = f_{Ph}(\mathbf{T}, T_z^h, t_s), \quad \forall z, t_s \quad (12)$$

$$P_z^c(t_s) = f_{Pc}(\mathbf{T}, T_z^c, t_s), \quad \forall z, t_s \quad (13)$$

$$\alpha, \lambda \geq 0, \quad (14)$$

$$\lambda \geq 1 \quad (15)$$

We have added a second term in Equation 8 to represent the violation of zone temperature constraints. $\max(T_{min} - T_z(t_s), T_z(t_s) - T_{max}, 0)$ is the max of violation of zone temperature of either below minimum and above maximum temperature. We also add two coefficients, α , which prioritizes reducing power consumption vs temperature comfort. Increasing α penalizes more on violating temperature constraints, and decreasing α will give more emphasis on energy reduction. α is constrained to be above 0 as in Equation 14, but with no upper limit. The reason being that the power consumption and temperature are of different scales and cannot be normalized to same range.

λ is a pre-determined constant that determines the penalty as a function of deviation of zone temperature from either minimum or maximum constraint. Increasing λ is exponentially increases penalty. It's constrained to be more than 1 as in Equation 15. An example of temperature penalty term for $\alpha = 1$ and $\lambda = 1.5$ is shown in Figure 1. Temperature delta refers to the delta by which zone temperature exceeding the temperature constraints.

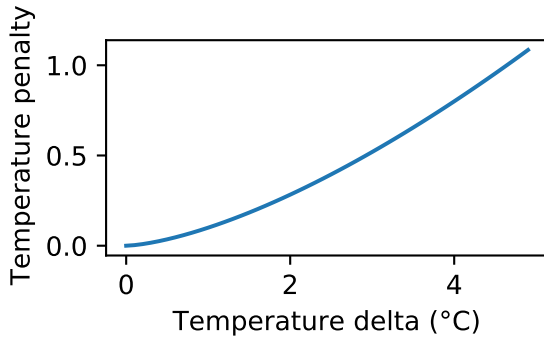


Figure 1: Temperature penalty curve adopted in our experiments.

In Equation 8, we added a new penalty coefficient α , which prioritizes reducing power consumption vs temperature comfort.

Increasing α penalizes more on violating temperature constraints, and decreasing α will give more emphasis on energy reduction. α is constrained to be above 0 as in Equation 14, but with no upper limit. The reason being that the power consumption and temperature are of different scales and cannot be normalized to same range. Rest of the equations remain same as Equations 2 – 6.

The following sections discuss the simulation engine we use for our experiment, and the co-simulation with DRL optimizers.

2.2 Ray RLLib and OpenAI Gym

RLLib [10] is a popular open-source library for reinforcement learning (RL) that is built on Ray [16]. RLLib offers highly scalability and packs many commonly used policies, e.g. PPO [21], DDPG [11], etc., for RL training. Gym [2] is a toolkit from OpenAI for developing reinforcement learning algorithms. Gym provides standard interfaces for initializing environment, where we define the action and observation spaces, functions for resetting environment, and providing controls and observing outputs at every time step of the simulation. RLLib interfaces with Gym seamlessly.

2.3 Co-simulation Routine

We combine EnergyPlus with a RL framework to co-simulate and determine the optimal settings for HVAC operation. A user can provide building information, e.g. HVAC system (heat sources, rate of cooling/heating, etc.), number of zones, building material, etc., in an input file called IDF. EnergyPlus reads the IDF file and the weather file to compute heating and cooling loads for every time step.

Co-simulation refers to synchronizing two or more simulations in parallel. In our case, it is the synchronization of reading observations from EnergyPlus, and generating action for next time step from RLLib. This turns out to be a challenge since RLLib and EnergyPlus runs on different processes. EnergyPlus provides support for BCVTB (Building Controls Virtual Test Bed), which is a software environment that allows users to couple different simulation programs for co-simulation. BCVTB uses Ptolemy server in the backend. This solution works, when one program is controlling one run of EnergyPlus, but with RLLib, it can spin multiple rollout workers, and each of them would need to start an EnergyPlus process. BCVTB based solution does not work in this scenario.

Fortunately, EnergyPlus from version 9.3 onward provides `pyenergyplus`, a Python library that contains callbacks to various states within EnergyPlus. Using this callbacks, we can intercept EnergyPlus, gather variables of interest, and pause the simulator until the necessary calculation needs to be done by RLLib. In order for RLLib to gather outputs from EnergyPlus and compute next action based on reward, we utilize the callback function `callback_end_zone_timestep_after_zone_reporting`, which returns to our Gym class at the end of every zone timestep after generating outputs. In this function, we collect outputs and put it in a queue, that will be picked by Gym step function, and compute the corresponding next action. Queues act as synchronization mechanism between our Gym environment and EnergyPlus. The framework is depicted in Figure 2.

In order to change the setpoints on every timestep, we add following constant schedules in building IDF:

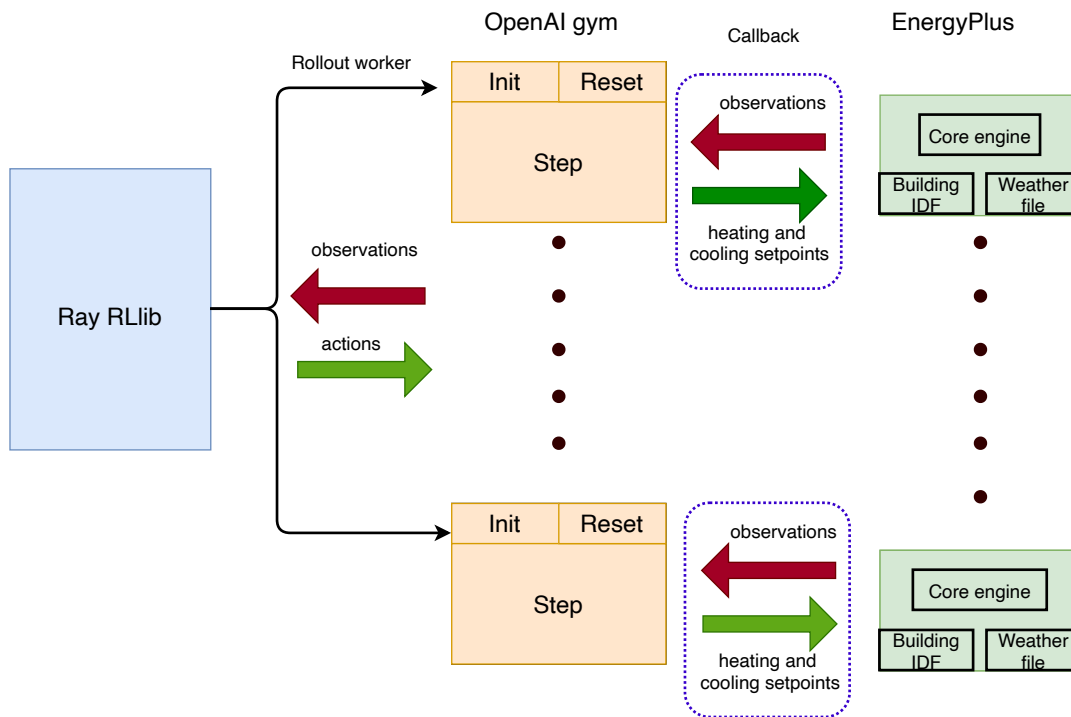


Figure 2: Distributed co-simulation framework involving Ray RLLib, OpenAI gym, and EnergyPlus

```
Schedule:Constant,
  CLGSETP_SCH_Perimeter_top_ZN_4,  !- Name
  Temperature,                    !- Schedule Type Limits Name
  20.0;                            !- Hourly Value
```

Through EnergyPlus callback, we modify this setpoint to desired setpoint, which will be held constant for the given timestep.

3 DEEP REINFORCEMENT LEARNING FOR BUILDING HVAC CONTROL

Reinforcement learning (RL) is a branch of machine learning that is specialized for solving control problems. Unlike classical control problems, where action is usually based on the immediate feedback, in many RL problems, the optimal policy could depend on delayed feedback, or need to discount current feedback. A RL problem primarily consists of following components:

- **State:** State is the mathematical description of the environment. For example, in the case of HVAC control of a building, state would represent the current temperatures and humidity in various zones of the building, outdoor environment temperature and humidity, heating and cooling loads, etc.
- **Action:** Action represents the control taken on the environment. In the example of HVAC control, action could be setting the thermostat setpoints for each zone, fan speeds, etc.
- **Agent:** The job of an agent is to compute an optimal action for a given state, under an optimal policy.

- **Environment:** Environment is the super set, where one or more actions, result in a state transition with associated observations. Each state transition has an associated transition probability that is dependent on the current state and the action taken. Depending on the objective, a reward function is used to predict immediate rewards for an action under a state.

The goal of an RL agent is to compute an optimal policy given a sequence of actions and subsequent observations. There are primarily two ways of achieving this goal:

- **Model-based RL:** Model-based RL is used in environments where we know the functions for transition probability and rewards are known. In this case, we can use policy or value iteration to find the optimal policy.
- **Model-free RL:** In most environments we don't know the exact characteristics of the environment. In that case, the controller needs to determine the optimal policy without modeling the environment. Policy gradient, value-based, and actor-critic are some of the common approaches used in model-free RL. We use model-free approach in this work.

3.1 DRL algorithms

Many algorithms for DRL have been developed over last few years. They can be divided based on several factors, e.g. whether the algorithm is improving same policy - on-policy, or continuously exploring new policies - off-policy; whether the algorithms support continuous or discrete control; if the algorithms are gradient

based or derivative free. We will discuss some of the popular DRL algorithms in this section that are also supported in RLlib.

PPO (Proximal Policy Optimization) [21] is a popular on-policy algorithm, which improves upon TRPO (Trust Region Policy Optimization) [20] by avoiding Kullback–Leibler divergence as a hard constraint, instead add the constraint as a penalty, which simplifies the computation. DDPG [11] is another model-free off-policy algorithm designed for learning continuous actions. DDPG uses Experience Replay and slow-learning target networks from DQN (Deep Q-Network) [14], and it is based on DPG (Deterministic Policy Gradient) [23].

Asynchronous Actor-Critic (A2C) and Advantage Actor-Critic (A3C) [13] methods updates the gradients asynchronously, which improves training times. Soft Actor Critic (SAC) [7] is an off-policy actor-critic DRL algorithm based on the maximum entropy reinforcement learning framework, where the actor aims to maximize expected reward while also maximizing entropy. Ape-X [8] provides a distributed architecture for DRL. When combined with DDPG, it can be used to scale across multiple instances.

3.2 Multi-zone HVAC Control

A building usually has multiple zones that could be spread over multiple floors. In a normal operation, these setpoints are set at a constant value. Since the range of desired temperature is a range, the zonal setpoints need not be set to a constant setpoint, but can be altered to match with external weather to reduce energy consumption. The setpoints for all zones could be set the same value, or they could be set independently to accommodate for differential temperatures between zones, e.g. core zones are less impacted by external weather than the perimeter zones. We will explore these options in detail in Section 4.3.

3.3 Multi-agent

In a multi-agent setting, multiple agents are making control decision on an environment. There are two ways of setting up a multi-agent problem:

- **Cooperative:** In this setting, agents share their observations, and might have a common reward. The idea behind this is to maximize rewards for all agents.
- **Competitive:** Here agents do not share their observation. They only try to maximize their individual rewards.

For our experiments, we consider cooperative type multi-agents. Specifically, we create two agents, one to control heating setpoint and another to control cooling setpoint. The intuition behind this is that each agent can create a separate model, so that agent responsible for setting heating setpoints can optimize for colder months, while the other agent can optimize for warmer months.

4 EXPERIMENTS

4.1 Setup

The following are some of the important settings we use in our experiments.

- **EnergyPlus:** v9.3.0

- **Building:** DOE Commercial Reference Building Medium office, new construction 90.1-2004 (RefBldgMediumOffice-New2004_Chicago.idf¹).
- **Weather file:** Toronto, Canada (CAN_ON_Toronto.716240_CWEC.epw²). We chose Toronto location, as it has good difference in temperature values between summer and winter months.
- **Simulation days:** We simulate for an entire year, i.e. 365 days. For comparison, we also simulate for 30 days in the month of January and July in Section 4.2.
- **Zones considered:** The reference building has three floors and each floor is subdivided into multiple core (center) and perimeter zones. The details of the zones and their names are listed in the next paragraph. We consider all of these zones.
- **Controls:** Heating and cooling setpoints for all zones.
- **Reward:** We use the reward defined in Equation 8.
- **Algorithms:** APEX_DDPG [11] and PPO [21].
- **RL library:** Amazon SageMaker RL footnote <https://docs.aws.amazon.com/sagemaker/latest/dg/reinforcement-learning.html> with Ray RLlib, version 1.0.
- **Deep learning framework:** PyTorch 1.8.1.
- **Python version:** 3.6.
- **Simulation timestep:** 15 minutes.
- **Desired range of zone temperatures:** 20°C – 25°C.
- **Heating setpoint range:** 15°C to 22°C.
- **Cooling setpoint range:** 22°C to 30°C.
- **Training instance:** ml.g4dn.16xlarge, which has 64 cores, 256 MB of RAM, and 1 NVIDIA T4 GPU.

The reference building has following 15 zones: Core_bottom, Core_mid, Core_top, Perimeter_bot_ZN_1, Perimeter_bot_ZN_2, Perimeter_bot_ZN_3, Perimeter_bot_ZN_4, Perimeter_mid_ZN_1, Perimeter_mid_ZN_2, Perimeter_mid_ZN_3, Perimeter_mid_ZN_4, Perimeter_top_ZN_1, Perimeter_top_ZN_2, Perimeter_top_ZN_3, and Perimeter_top_ZN_4. Core refers to the center of a floor, perimeter refers to the zones on the periphery of a floor. ‘top’, ‘mid’, and ‘bottom’ refers to the location of the floors.

In addition to zone temperatures, we use following observations:

- **Air System Total Heating Energy**, which is heat added to the air loop (sum of all components) in Joules. Similarly, **Air System Total Cooling Energy** is heat removed from the air loop. These variables are collected for each VAV (variable air volume) 1, 2, and 3. Their sum is represented as P_z^h and P_z^c in Table 1, respectively. VAV is a type of HVAC system, which unlike constant air volume systems can vary the airflow at a constant temperature.
- **Site Outdoor Air Wetbulb Temperature** and **Site Outdoor Air Drybulb Temperature**. Dry-bulb temperature is the temperature that measures air temperature without the effect of any moisture. On the other hand, wet-bulb temperature is the lowest temperature that can be reached

¹<https://bcl.nrel.gov/node/85021>

²https://energyplus.net/weather-location/north_and_central_america_wmo_region_4/CAN/ON/CAN_ON_Toronto.716240_CWEC

under current ambient conditions by the evaporation of water only. Since wet-bulb temperature accounts for relative humidity, we include that as one of the observables.

In the following sections, we will explore the effect of various configurations on the reward optimization and training times.

4.2 Effect of α and Seasons on Reward

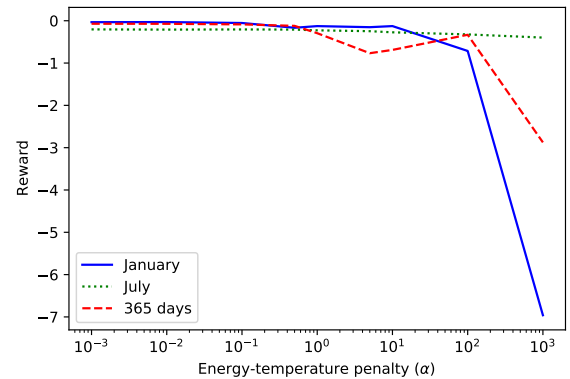
As described earlier, α controls if we are optimizing more for energy savings vs temperature comfort. The final reward of a simulation depends not only on α , but also on the number of simulation days, and the seasons captured in the simulation run. Since the rewards generated for every time step are accumulated towards final reward, we need to normalize the rewards for number of simulation days. Figure 3 shows the comparison of reward function, energy consumption, and mean violation of zone temperatures for various α , when simulated for 30 days in the months of January and July, and also for entire year (365 days). January and July were chosen as these two months are representative of cold and warm months in a typical climate. The raw data points are provided in Table 4 in the Appendix A.1.

From the plots, we see that in general, energy consumption is higher in winter, as the differential between external temperature and the indoor temperature is higher in winter than in summer (for Toronto region). Similar reasoning also applies for mean temperature violation, where we see higher violation for January month than for July. Simulating for entire year tries to find a policy that works for both seasons, and ends up not being best in both seasons. It is for this reason, we explore using multi-agent policy (Section 4.5), where one policy focuses on warmer months, while other on colder months.

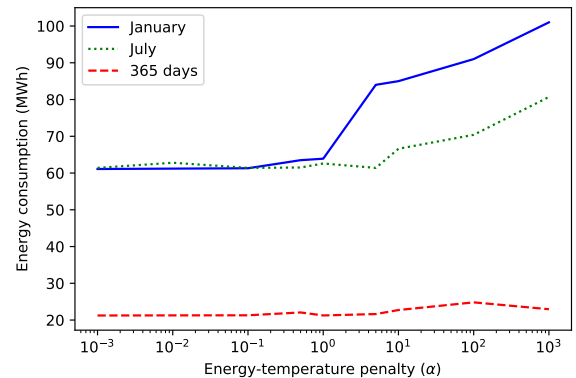
Comparison with baseline: In addition to above experiment, we simulated the baseline experiment, where we set the heating setpoint to 20°C and cooling setpoint to 22.5°C for all zones, as they are the minimum values to avoid temperature violation yet, and thus minimize energy consumption. The result was the total baseline energy is 517.41 MWh and mean temperature violation is 0.118 °C. Comparing with centralized policy, we see that RL algorithms at the minimum (for $\alpha = 0.001$) gives 75% reduction in energy consumption and mean temperature lower is by 0.116 °C.

4.3 Multi-zone

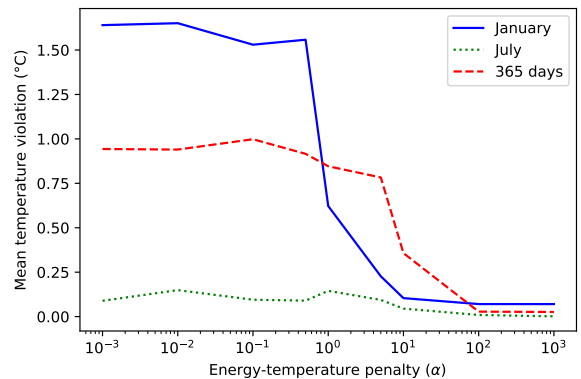
There are two approaches in controlling HVAC of a building - one is centralized control, where every zone gets same heating and cooling setpoint at a given time, the other is individualized control for each zone. We evaluate the rewards for various α , and energy consumption and mean temperature violation for above approaches. These observations are summarized in Figure 4. From the figure, we see that multi-zone approach does better in overall reward value, energy consumption, and also on mean temperature violation over the entire range of α . For couple of datapoints, centralized policy seems to be doing better than multi-zone. This cross-over value is small and we believe it could be due to random nature of policy optimization. This agrees with our intuition that different zones in a building need different temperature setting as all zones don't have same thermal dynamics, e.g. a perimeter zone on south side will receive more sun than the core zones, and thus would need a



(a) Plot of final reward.



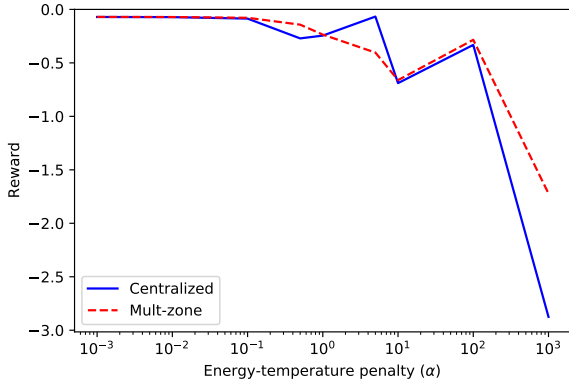
(b) Plot of energy consumption. The energy consumption of 365 days simulation is normalized for 30 days for comparison reasons.



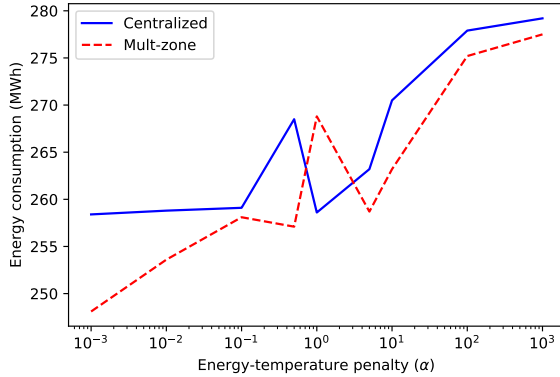
(c) Plot of mean temperature violation.

Figure 3: Plot showing the effect of number of simulation days and season on the reward for various α .

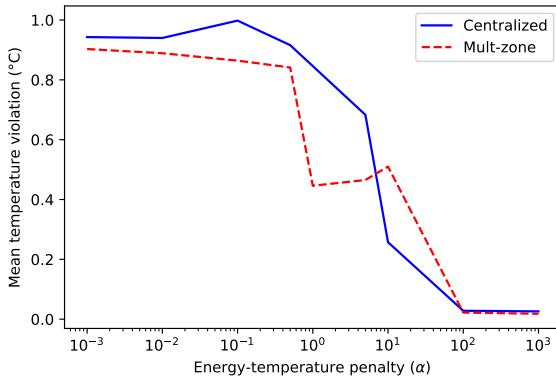
different setpoint than the core zones. Please refer to Appendix A.2 for raw data used in the plots.



(a) Plot of final reward.



(b) Plot of energy consumption.



(c) Plot of mean temperature violation.

Figure 4: Plot comparing multi-zone policy vs centralized policy for various α .

4.4 Impact of Weather on HVAC Optimization

In this section, we consider the impact of external weather on HVAC optimization of a building. We use weather from 6 locations

and perform multi-zone optimization as described in the previous section. Figure 5 describes the plots of reward, energy consumption, and mean temperature violation for different locations. The average temperature and humidity for entire year for each location, along with temperature difference between summer and winter months are overlay on the plots for better understanding. The details of data and full names of location can be found in Appendix A.3.

From the plots, we see that the average external temperature plays a big role in reducing energy consumption, which also impact the reward. Both low and high average temperatures decreases reward (see Toronto and Tampa, FL), as that would require more energy to keep indoor temperature in the comfort zone. Note that the x-axis in Figure 5a is inverted. The lower the bar, better the reward value. In general, it takes more energy to cool than to heat, as we can see from Figure 5b, where higher average temperatures in Tampa, FL requires more than double the energy consumption for a building to cool than for a building in Toronto, where the temperatures on average are much cooler.

Mean difference in summer and winter temperatures also plays a role, as it represents the differential work, the HVAC systems need to do to keep indoor temperatures within comfort zone, across different seasons. Similarly, higher humidity keeps the outdoor temperatures relatively constant, which reduces mean temperature violation in zones, as see with San Francisco location.

4.5 Multi-agent

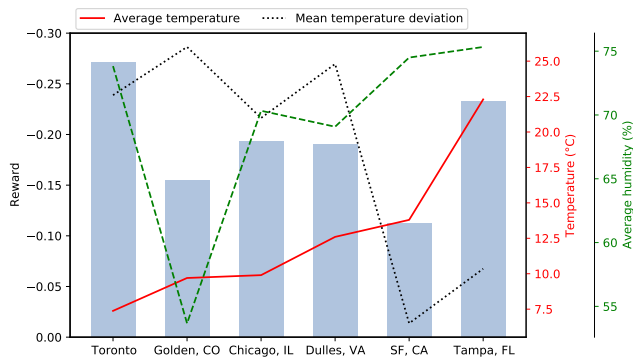
Next, we explored setting up multiple agents to control HVAC. The idea behind multi-agent control is that multiple agents may better optimize reward, when the controls are not homogeneous. For example, in HVAC use case, we have two sets of controls - heating setpoint and cooling setpoint. Heating setpoint is used during winter months to increase indoor temperature, while cooling setpoint is used in summer months to reduce indoor temperature. A single agent will model the environment using a single neural network and uses same weights to decide next heating setpoint and cooling setpoint controls, which may not be optimal. With multi-agent, each agent (heating/cooling setpoint) will optimize individual network for the control they are responsible. Figure 6 compares multi-agent policy with multi-zone policy we discussed earlier. From the figure, we notice that multi-agent does better than multi-zone in general across various α .

4.6 Comparison of RL Algorithms

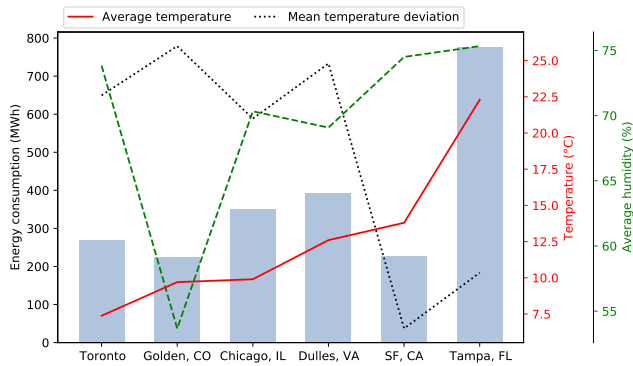
In this experiment, we compare two RL algorithms PPO and APEX-DDPG that were described in Section 3.1. Table 2 and Figure 7 summarizes the comparison of different algorithms mentioned above. Rewards from PPO (for different observation filters) and APEX-DDPG are close. In terms of training times, APEX-DDPG has the lowest training time (60% lower than PPO) and the reward converges in 84% less iterations. MeanStdFilter, which keeps track of running mean, took longer to converge and with no significant improvement in reward.

4.7 Training Cost Optimization

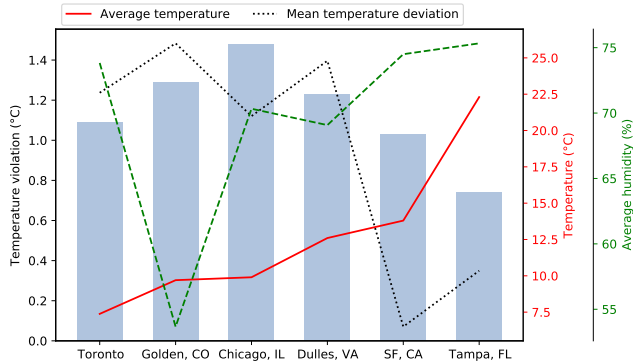
In the final experiment, we run our HVAC optimization on different AWS instances as listed in Table 3. The table lists GPU types if the



(a) Plot of final reward.



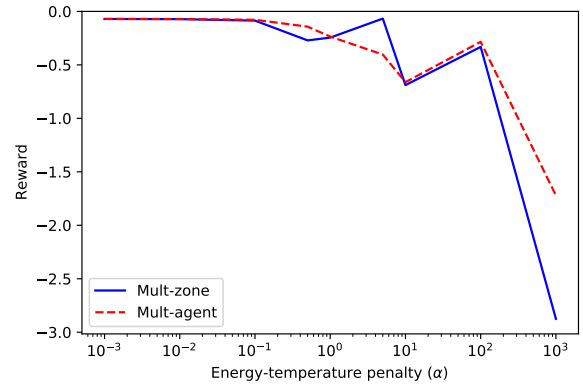
(b) Plot of energy consumption.



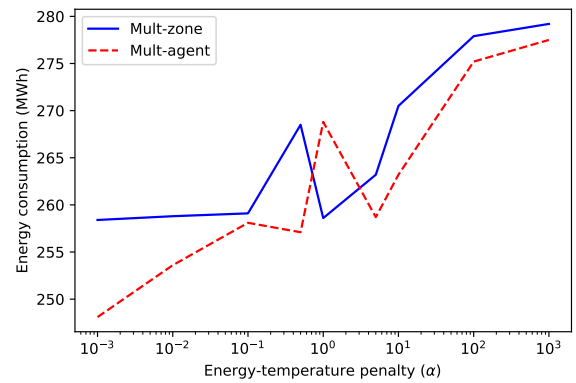
(c) Plot of mean temperature violation.

Figure 5: Plot of impact of external weather on HVAC optimization. Each plot contains metrics for 6 cities along with plot of average temperature, average humidity, and mean temperature deviation from summer and winter months. α was set to 1.

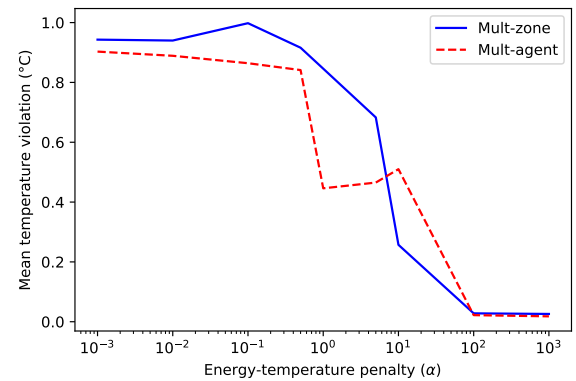
instances have a GPU, number of CPU cores, the training time, and the resulting cost. From the table, we can infer that having many cores is very helpful to rollout many RLlib workers, at the same time having a low cost GPU is useful to train the model in less time. For our experiments, we found ml.g4dn.16xlarge turns to be the low cost.



(a) Plot of final reward. Note the x-axis is inverted. The smaller the length of the bar, better the reward.



(b) Plot of energy consumption.

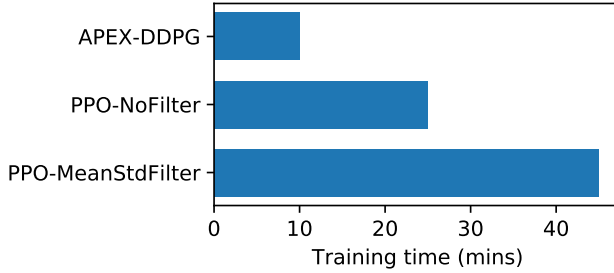


(c) Plot of mean temperature violation.

Figure 6: Plot comparing multi-zone with multi-agent policies for various α .

Table 2: Table comparing RL algorithms along with different configuration values, in terms of reward value and training time .

Algorithm	Observation filter	Reward	Iteration count	Training time (s)
PPO	NoFilter	-293.19	104	25
	MeanStdFilter	-292.73	178	45
APEX-DDPG	-	-293.02	17	10

**Figure 7: Plot comparing training times for PPO (NoFilter and MeanStdFilter observation filters) and APEX-DDPG algorithms.****Table 3: Table comparing convergence times on different instances on Amazon SageMaker and their respective costs.**

Instance type	GPU type	CPU cores	Training time (mins)	Training cost (\$)
ml.g4dn.16xlarge	T4	64	15	1.36
ml.p3.2xlarge	V100	8	40	2.55
ml.p2.xlarge	K80	4	135	2.53
ml.c5.18xlarge	-	72	35	2.14
ml.m5.24xlarge	-	96	50	4.6

5 CONCLUSION

In this paper, we have presented a scalable framework for optimizing HVAC on a commercial building using deep reinforcement learning. We have conducted experiments, showing the impact of simulation days, weather, energy-temperature penalty coefficient on the reward. We have also shown how to set up multi-zone and multi-agent control in this framework. We believe this framework will ease the adoption of DRL in HVAC optimization with researchers and practitioners, and spur further innovation.

REFERENCES

- [1] Ercan Atam and Lieve Helsens. 2016. Control-Oriented Thermal Modeling of Multizone Buildings: Methods and Issues: Intelligent Control of a Building System. *IEEE Control Systems Magazine* 36, 3 (2016), 86–111.
- [2] Greg Brockman, Vicki Cheung, Ludwig Pettersson, Jonas Schneider, John Schulman, Jie Tang, and Wojciech Zaremba. 2016. OpenAI Gym. *CoRR* abs/1606.01540 (2016).
- [3] Yize Chen, Yuanyuan Shi, and Baosen Zhang. 2019. Optimal Control Via Neural Networks: A Convex Approach. arXiv:1805.11835 [math.OC]

- [4] Drury B. Crawley, Linda K. Lawrie, Frederick C. Winkelmann, W.F. Buhl, Y. Joe Huang, Curtis O. Pedersen, Richard K. Strand, Richard J. Liesen, Daniel E. Fisher, Michael J. Witte, and Jason Glazer. 2001. EnergyPlus: creating a new-generation building energy simulation program. *Energy and Buildings* 33, 4 (2001), 319–331.
- [5] Guanyu Gao, Jie Li, and Yonggang Wen. 2019. Energy-Efficient Thermal Comfort Control in Smart Buildings via Deep Reinforcement Learning. arXiv:1901.04693 [cs.SY]
- [6] Guang Geng and G.M. Geary. 1993. On performance and tuning of PID controllers in HVAC systems. In *Proceedings of IEEE International Conference on Control and Applications*, Vol. 2. 819–824.
- [7] Tuomas Haarnoja, Aurick Zhou, Kristian Hartikainen, George Tucker, Sehoon Ha, Jie Tan, Vikash Kumar, Henry Zhu, Abhishek Gupta, Pieter Abbeel, and Sergey Levine. 2019. Soft Actor-Critic Algorithms and Applications. arXiv:1812.05905 [cs.LG]
- [8] Dan Horgan, John Quan, David Budden, Gabriel Barth-Maroon, Matteo Hessel, Hado van Hasselt, and David Silver. 2018. Distributed Prioritized Experience Replay. arXiv:1803.00933 [cs.LG]
- [9] M. Killian and M. Kozek. 2016. Ten questions concerning model predictive control for energy efficient buildings. *Building and Environment* 105 (2016), 403–412.
- [10] Eric Liang, Richard Liaw, Philipp Moritz, Robert Nishihara, Roy Fox, Ken Goldberg, Joseph E. Gonzalez, Michael I. Jordan, and Ion Stoica. 2018. RLlib: Abstractions for Distributed Reinforcement Learning. arXiv:1712.09381 [cs.AI]
- [11] Timothy P. Lillicrap, Jonathan J. Hunt, Alexander Pritzel, Nicolas Heess, Tom Erez, Yuval Tassa, David Silver, and Daan Wierstra. 2019. Continuous control with deep reinforcement learning. arXiv:1509.02971 [cs.LG]
- [12] Xiaoshu Lü, Tao Lu, Charles J. Kibert, and Martti Viljanen. 2015. Modeling and forecasting energy consumption for heterogeneous buildings using a physical-statistical approach. *Applied Energy* 144 (2015), 261–275.
- [13] Volodymyr Mnih, Adrià Puigdomènech Badia, Mehdi Mirza, Alex Graves, Timothy P. Lillicrap, Tim Harley, David Silver, and Koray Kavukcuoglu. 2016. Asynchronous Methods for Deep Reinforcement Learning. arXiv:1602.01783 [cs.LG]
- [14] Volodymyr Mnih, Koray Kavukcuoglu, David Silver, Alex Graves, Ioannis Antonoglou, Daan Wierstra, and Martin Riedmiller. 2013. Playing Atari with Deep Reinforcement Learning. arXiv:1312.5602 [cs.LG]
- [15] Volodymyr Mnih, Koray Kavukcuoglu, David Silver, Andrei A. Rusu, Joel Veness, Marc G. Bellemare, Alex Graves, Martin Riedmiller, Andreas K. Fiedelnd, Georg Ostrovski, Stig Petersen, Charles Beattie, Amir Sadik, Ioannis Antonoglou, Helen King, Dharmashan Kumaran, Daan Wierstra, Shane Legg, and Demis Hassabis. 2015. Human-level control through deep reinforcement learning. *Nature* 518, 7540 (01 Feb 2015), 529–533.
- [16] Philipp Moritz, Robert Nishihara, Stephanie Wang, Alexey Tumanov, Richard Liaw, Eric Liang, Melih Elilob, Zongheng Yang, William Paul, Michael I. Jordan, and Ion Stoica. 2018. Ray: A Distributed Framework for Emerging AI Applications. arXiv:1712.05889 [cs.DC]
- [17] Takao Moriyama, Giovanni De Magistris, Michiaki Tatsubori, Tu-Hoa Pham, Asim Munawar, and Ryuki Tachibana. 2018. Reinforcement Learning Testbed for Power-Consumption Optimization. In *Methods and Applications for Modeling and Simulation of Complex Systems*, Liang Li, Kyoko Hasegawa, and Satoshi Tanaka (Eds.). Springer Singapore, 45–59.
- [18] U.S. Department of Energy. [n.d.]. *Buildings Energy Data Book*.
- [19] Samuel Privara, Zdeněk Váňa, Dimitrios Gyalistras, Jiří Cigler, Carina Sager-schnig, Manfred Morari, and Lukáš Ferkl. 2011. Modeling and identification of a large multi-zone office building. In *2011 IEEE International Conference on Control Applications (CCA)*. 55–60.
- [20] John Schulman, Sergey Levine, Philipp Moritz, Michael I. Jordan, and Pieter Abbeel. 2017. Trust Region Policy Optimization. arXiv:1502.05477 [cs.LG]
- [21] John Schulman, Filip Wolski, Prafulla Dhariwal, Alec Radford, and Oleg Klimov. 2017. Proximal Policy Optimization Algorithms. arXiv:1707.06347 [cs.LG]
- [22] Pervez Hameed Shaikh, Nursyarizal Bin Mohd Nor, Perumal Nallagownden, Irraivan Elamvazuthi, and Taib Ibrahim. 2014. A review on optimized control systems for building energy and comfort management of smart sustainable buildings. *Renewable and Sustainable Energy Reviews* 34 (2014), 409–429.
- [23] David Silver, Guy Lever, Nicolas Heess, Thomas Degris, Daan Wierstra, and Martin Riedmiller. 2014. Deterministic Policy Gradient Algorithms. In *Proceedings of the 31st International Conference on International Conference on Machine Learning - Volume 32 (Beijing, China) (ICML '14)*. JMLR.org, 1–387–1–395.
- [24] Richard S. Sutton and Andrew G. Barto. 2018. *Reinforcement Learning: An Introduction*. A Bradford Book.
- [25] Tianshu Wei, Yanzi Wang, and Qi Zhu. 2017. Deep reinforcement learning for building HVAC control. In *2017 54th ACM/EDAC/IEEE Design Automation Conference (DAC)*. 1–6.
- [26] Zhiang Zhang, Adrian Chong, Yuqi Pan, Chenlu Zhang, and Khee Poh Lam. 2019. Whole building energy model for HVAC optimal control: A practical framework based on deep reinforcement learning. *Energy and Buildings* 199 (2019), 472–490.

Table 4: Table with results on simulation of effect of energy-temperature penalty coefficient (α), duration of simulation, and the month of simulation on reward value.

α	Reward			Energy consumption(MWh)			Mean temperature violation ($^{\circ}$ C)		
	January (30)	July (30)	Year (365)	January (30)	July (30)	Year (365)	January (30)	July (30)	Year (365)
0.001	-0.034	-0.2045	-0.0709	61.1	61.4	21.2	1.64	0.089	0.943
0.01	-0.0313	-0.2095	-0.0721	61.2	61.4	21.3	1.651	0.149	0.94
0.1	-0.0532	-0.2055	-0.0861	61.3	62.8	21.3	1.53	0.095	0.998
0.5	-0.166	-0.209	-0.121	63.5	61.4	22.1	1.558	0.0898	0.916
1	-0.1267	-0.2267	-0.2943	63.9	61.5	21.3	0.622	0.145	0.846
5	-0.1523	-0.2468	-0.767	84	62.6	21.6	0.227	0.094	0.783
10	-0.1263	-0.2733	-0.6893	85	22.7	276.5	0.104	0.045	0.3571
100	-0.714	-0.323	-0.3318	91	24.8	301.9	0.071	0.0092	0.028
1000	-6.96	-0.398	-2.875	101	22.9	279.2	0.0704	0.0015	0.0261

A DATA USED IN PLOTS GENERATION

In this appendix, we will provided detailed data that was used to generate plots in Section 4.

A.1 Effect of α and Seasons on Reward

Table 4 provides the data used for generating Figure 3.

A.2 Comparison of Centralized vs Multi-zone Control

Table 5 provides the data used for generating Figure 4.

Table 5: Table comparing centralized vs multi-zone control on reward value and training time as α is varied.

Control type	α	Energy consumption (MWh)	Mean temperature violation ($^{\circ}$ C)	Reward
Centralized	0.001	265.5	1.422	-0.073
	0.01	266.2	1.287	-0.075
	0.1	264.8	1.395	-0.098
	0.5	264.8	1.395	-0.298
	1	274.4	1.14	-0.276
	5	265.4	0.568	-0.851
	10	272.6	0.2131	-0.4215
	100	276.9	0.497	-5.492
	1000	289	0.02	-2.053
	Multi-zone	0.001	258.4	0.943
0.01		258.8	0.94	-0.0721
0.1		259.1	0.998	-0.0861
0.5		268.5	0.916	-0.121
1		258.6	0.846	-0.2943
5		263.2	0.783	-0.767
10		276.5	0.3571	-0.6893
100		301.9	0.028	-0.3318
1000		279.2	0.0261	-2.875

A.3 Impact of Weather on HVAC Optimization

Table 6 provides the data used for generating Figure 5. The following are the full names of the location found in NREL website.

- CAN_ON_Toronto.716240_CWEC
- USA_FL_Tampa.Intl.AP.722110_TMY3
- USA_CA_San.Francisco.Intl.AP.724940_TMY3
- USA_CO_Golden-NREL.724666_TMY3
- USA_IL_Chicago-OHare.Intl.AP.725300_TMY3
- USA_VA_Sterling-Washington.Dulles.Intl.AP.724030_TMY3

Table 6: Table comparing centralized vs multi-zone control on reward value and training time as α is varied.

Location	Energy consumption (MWh)	Mean temperature violation ($^{\circ}$ C)	Reward	Average temperature ($^{\circ}$ C)	Humidity (%)	Mean weather temperature deviation ($^{\circ}$ C)
Toronto	269.3	1.088	-0.271	7.38	73.83	22.6
Golden, CO	224.9	1.287	-0.1544	9.7	53.67	26
Chicago, IL	350.1	1.48	-0.1929	9.9	70.33	20.99
Dulles, VA	393.5	1.231	-0.1901	12.6	69.08	24.8
San Francisco, CA	227.3	1.032	-0.1128	13.8	74.5	6.5
Tampa, FL	777.1	0.742	-0.233	22.3	75.33	10.35

A.4 Comparison of Single vs Multi-agent

Table 7 provides the data used for generating Figure 6.

Table 7: Table comparing multi-zone vs. multi-agent policies on reward value, energy consumption, mean temperature violation, as α is varied.

Control type	α	Energy consumption (MWh)	Mean temperature violation ($^{\circ}\text{C}$)	Reward)
Multi-zone	0.001	258.4	0.943	-0.0709
	0.01	258.8	0.94	-0.0721
	0.1	259.1	0.998	-0.0861
	0.5	268.5	0.916	-0.121
	1	258.6	0.846	-0.2943
	5	263.2	0.783	-0.767
	10	276.5	0.3571	-0.6893
	100	301.9	0.028	-0.3318
	1000	279.2	0.0261	-2.875
Multi-agent	0.001	248.1	0.903	-0.0702
	0.01	253.6	0.889	-0.0712
	0.1	258.1	0.8642	-0.0784
	0.5	257.1	0.8413	-0.1425
	1	268.8	0.446	-0.2355
	5	258.7	0.4652	-0.4036
	10	263.2	0.51	-0.6612
	100	275.2	0.022	-0.2841
	1000	277.5	0.018	-1.7213